

# Learning to Estimate 6DoF Pose from Limited Data: A Few-Shot, Generalizable Approach using RGB Images

Panwang Pan<sup>1\*</sup>, Zhiwen Fan<sup>2\*</sup>, Brandon Y. Feng<sup>3\*</sup>, Peihao Wang<sup>2\*</sup>, Chenxin Li<sup>4</sup>, Zhangyang Wang<sup>2</sup>  
<sup>1</sup>ByteDance, <sup>2</sup>University of Texas at Austin,  
<sup>3</sup>University of Maryland, <sup>4</sup>Hong Kong Polytechnic University

## Abstract

The accurate estimation of six degrees-of-freedom (6DoF) object poses is essential for many applications in robotics and augmented reality. However, existing methods for 6DoF pose estimation often depend on CAD templates or dense support views, restricting their usefulness in real-world situations. In this study, we present a new cascade framework named **Cas6D** for few-shot 6DoF pose estimation that is generalizable and uses only RGB images.

To address the false positives of target object detection in the extreme few-shot setting, our framework utilizes a self-supervised pre-trained ViT to learn robust feature representations. Then, we initialize the nearest top- $K$  pose candidates based on similarity score and refine the initial poses using feature pyramids to formulate and update the cascade warped feature volume, which encodes context at increasingly finer scales. By discretizing the pose search range using multiple pose bins and progressively narrowing the pose search range in each stage using predictions from the previous stage, **Cas6D** can overcome the large gap between pose candidates and ground truth poses, which is a common failure mode in sparse-view scenarios. Experimental results on the LINEMOD and GenMOP datasets demonstrate that **Cas6D** outperforms state-of-the-art methods by 9.2% and 3.8% accuracy (Proj-5) under the 32-shot setting compared to **OnePose++** and **Gen6D**. Our framework also performs best under the full-shot setting with all support views. The code will be released.

## 1. Introduction

Six degrees-of-freedom (6DoF) object pose estimation predicts the orientation and location of a target object in 3D space, which is a necessary preliminary step for downstream applications like robotic manipulation, augmented reality, and autonomous driving. However, traditional methods [45, 95, 104, 109, 51, 74, 46] often require instance-

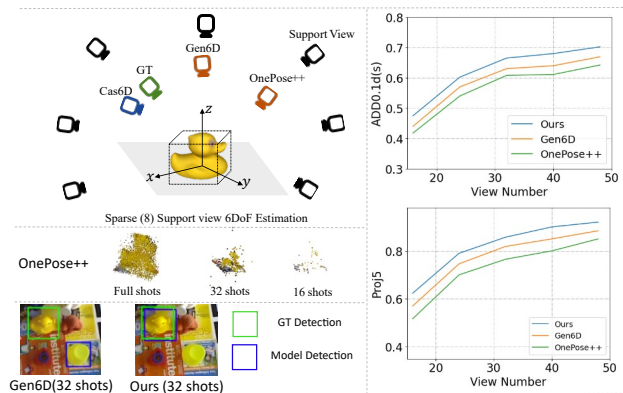


Figure 1. **Generalizable 6DoF Estimation from Sparse RGB Views without CAD Models.** While **OnePose++** [34] (middle left) and **Gen6D** [58] (bottom left) achieve promising accuracy given sufficient support views, their performance significantly degrades when few views are available. In contrast, **Cas6D** bridges the performance gap (+3.8% on Proj-5) on few-shot settings (right) without the need for depth maps or per-instance re-training.

level CAD models as prior knowledge, which can be difficult or impossible to obtain for objects in the wild. While category-level methods [98, 3, 17] eliminate the need for instance-level CAD models, they are limited to handling different instances within the same category and cannot generalize to unseen categories. To overcome these limitations, generalizable (model-free) methods, **OnePose** [92] and **OnePose++** [34] propose a one-shot object pose estimation method that can be used in arbitrary scenarios, which first reconstructs sparse object point clouds and then establishes 2D-3D correspondences between keypoints in the query image and the point cloud to estimate the object pose. Another recent method, **Gen6D** [58], uses a set of support views to detect the target object in a query image, selects a support view with the most similar appearance to provide the initial pose, and then refines the pose estimation using a feature volume constructed from 2D features.

Previous methods have shown good generalizability to new instances, but require dense support views at inference (e.g.,  $\geq 128$ ) which limits their effectiveness in real-

\*Equal contribution

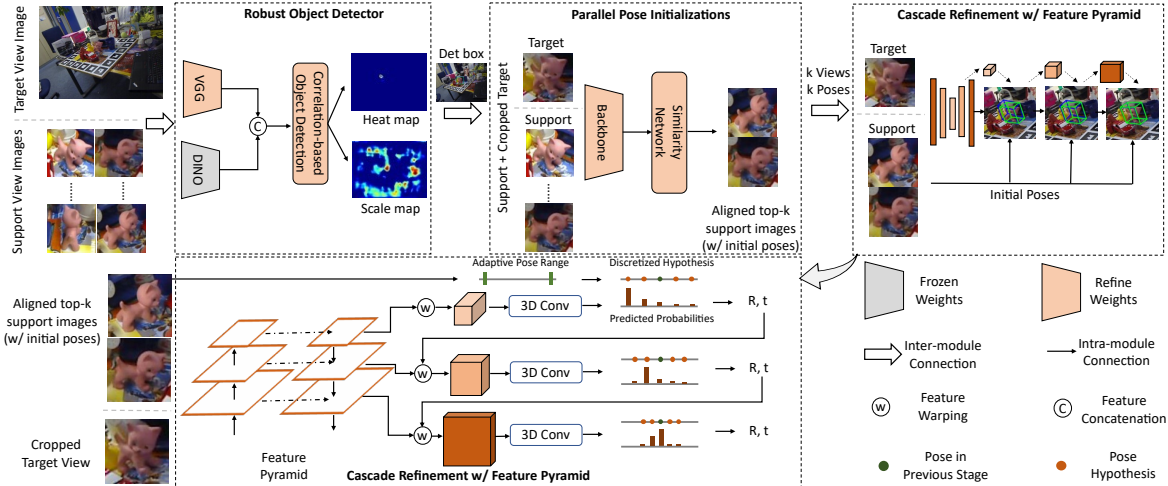


Figure 2. **The Overall Pipeline of the Proposed Cas6D Framework.** Given multi-view object images in support views and a target view image, our pipeline consists of three stages. Firstly, we detect and crop the object by localizing the heat and scale maps (top left). Secondly, we use a similarity network to find the best top-K aligned support images as pose initializations. Finally, we use the cascade pose refiner with feature pyramid to progressively estimate the pose residual by narrowing the search range.

world applications where images are often non-uniform and sparse [68]. This can result in a failure to reconstruct the point cloud with sparse viewpoints (e.g., OnePose++ [34]) or detect an accurate box (e.g., Gen6D [58]), leading to a large gap between the initial pose and ground truth poses, which are illustrated in Figure 1. While recent work, FS6D [35], has introduced a large-scale synthetic dataset to address this issue, it still requires depth maps as input, which is a significant constraint for real-world applications.

Can we design an efficient RGB-based 6DoF pose estimator without requiring additional 3D information (e.g., CAD model, depth map) under sparse support views? In this paper, we propose Cas6D, a novel CAD model-free solution for efficient RGB-based 6DoF pose estimation under sparse support views. Our approach leverages features extracted by the self-supervised ViT representation [12] to identify the correspondences for object parts [4] across views and thus detect the object in the target view. Then, we use a similarity network to find the top-K best-matched support images as pose initializations. To bridge the large gap between the initial poses and the sparse ground truth, we propose a cascaded coarse-to-fine refinement module. During training, we determine the initial pose gap and sample multiple pose hypotheses using a low-resolution feature volume based on coarse but semantic-rich 2D features. In later stages, we utilize pose estimates from earlier stages to adjust the sampling range of pose hypotheses and construct feature volumes of higher resolution with finer 2D semantic features. This framework allows for adaptive pose sampling with adjustable feature pyramids, which avoids using a single-scale 3D volume and ensures computational and memory resource efficiency.

Experiments on the LINEMOD [37] and GenMOP [58] datasets, show that Cas6D consistently outperforms other RGB-based generalizable and instance-wise methods. We summarize the contributions as follows:

- We address the challenging setting of few-shot, generalizable 6D object pose estimation using only RGB images. Our proposed Cas6D framework progressively estimates the pose of the target view from a limited number of support views.
- Our framework leverages representations extracted from a self-supervised pre-trained ViT network and employs a top-K pose proposals scheme for robust pose initialization. It also introduces a cascaded coarse-to-fine refinement procedure that uses feature pyramids and adaptively discrete pose hypotheses.
- We extensively evaluate our method on the widely used LINEMOD and GenMOP benchmarks, demonstrating that Cas6D outperforms previous state-of-the-art methods OnePose++ by 9.2%/4.7% and Gen6D by 3.8%/2.8%, measured by ADD-0.1d/Prj-5 metrics.

## 2. Related Works

**Generalizable Object Pose Estimator.** Recent advances in generalizable pose estimators aim to address the limitations of prior instance-specific methods [104, 94, 40, 74, 46, 41, 39, 42, 46, 102, 23, 57, 89, 78, 90, 108] which typically utilize CAD models or depth maps and category-specific [98, 17, 101, 22, 52, 17, 16, 53, 96, 24, 30] methods that require per-category training, enabling pose esti-

mation generalizing to unseen objects and categories. Depending on whether a 3D model is required, existing literature on generalizable pose estimation could be divided into two streams: model-based and model-free. The former requires high-quality object models either for shape embedding [105, 75, 20], template matching [36, 6, 103, 93], rendering-and-comparison approaches [50, 109, 70, 9]. To avoid the reliance on 3D models, the latter model-free methods utilize advanced neural rendering to directly render from posed images for pose estimation [107, 72, 55]. But some methods still assume the availability of depth maps [72] or object masks [107, 72, 55]. Besides, the iterative optimization process [107] is time-consuming and the work [55] introduce instant-ngp [66] as neural renderer with parallelized Monte Carlo sampling to mitigate the speed limitation. Other model-free methods such as Gen6D [58], OnePose [92] and OnePose++ [34], use only a set of reference/support images with annotated poses for the pose estimation of the object in the target image. Specifically, Gen6D [58] first detects the object box in the target view, initializes a pose from dense support views and refines the pose using feature volume and multiple 3D convolution layers. OnePose series [92, 34] first reconstruct the sparse point cloud from the RGB sequences of all support viewpoints, and match the target view with the sparse point cloud to determine the object poses. However, the above method easily fails under sparse view scenarios as Gen6D [58] may detect the incorrect box and fail to refine the pose due to large gap between initial and GT poses. OnePose series [92, 34] are not able to build high-quality point clouds due to sparse support view. As a comparison, we leverage the rich semantic prior from pre-trained ViT models (e.g., DINO-ViT [12]) for the accurate detection of an arbitrary object. We initialize multiple parallel poses from sparse support views based on the similarity scores, and progressively refine the object pose with cascade feature pyramid volumes and discrete pose hypotheses.

**Few-shot Learning in 3D Vision.** Few-shot learning is to develop a model that can generalize to new classes with very few examples, through meta-learning approaches [26, 28, 67, 80] or metric-based fashion [28, 88, 97]. For 6D pose estimation, the few-shot pose estimator usually employs local image feature matching [59], establishing correspondences between two images in a detector-based [61, 62, 82, 83] or detector-free [49, 56, 81, 91] fashion. Other methods leverage point cloud registration algorithms [77], which detect 3D keypoints [5, 48], extract feature descriptors [19, 21, 29, 38, 76], and estimate relative transformations [50]. The recently proposed FS6D [35] further leverages complementary depth information in RGBD input images for dense prototype extraction and matching. In comparison, our few-shot estimator leverages only RGB images, extending the applicable scenario to where depth in-

formation of objects is unavailable.

**Coarse-to-fine Estimation in 3D Vision.** Coarse-to-fine estimation is a widely adopted strategy in 3D vision, where the estimation process is gradually refined in multiple stages, each with an increasing level of precision. ZebraPose [90] proposes a coarse to fine training strategy to enable fine-grained correspondence prediction. Gen6D [58] first finds the closest support view and then refines the initial pose using feature volume and 3D convolutional layers. Several coarse-to-fine multi-view stereo works [32, 15, 18, 106] estimate a coarse depth map and then gradually recover details based on feature pyramid. Neural Radiance Field (NeRFs) [65, 7] uniform sample along each ray to determine the rough density field and perform importance sample in the later stages.

**Self-supervised Feature Representation.** Self-supervised learning is a well-studied topic in machine learning and computer vision [63, 71, 79, 87], with various methods for learning representations, such as clustering [8, 11, 43], GANs [73, 64], pretext tasks [25, 69, 100], etc. For 3D vision, most methods of self-supervised learning focus on single object representation with different applications to reconstruction, classification or part segmentation [2, 1, 27, 31, 33, 44, 47, 84]. Recent MVSFormer [10] proposes a pre-trained ViT-enhanced MVS network, which learns more reliable feature representations benefited by informative priors from self-supervised ViT. Inspired by this work, in this paper, we study whether self-supervised ViT can facilitate feature learning in a similar task as 6D pose estimation.

### 3. Methods

**Overview.** Given  $N_s$  RGB images (support views) of an object with known camera poses  $\{\mathbf{I}^{(i)}, \mathbf{p}^{(i)}\}_{i=1}^{N_s}$ , Cas6D predicts the object pose in the target view. Cas6D first detects the object box in the target view, finds the top- $K$  best-matched viewpoints to initialize the  $K$  poses, and conducts a coarse-to-fine refinement step using cascade feature volume and discrete pose hypotheses.

#### 3.1. Preliminary

**Generalizable 6DoF Estimation Framework** In the model-free OnePose series [92, 34], object poses are determined by reconstructing a sparse point cloud from RGB sequences of support viewpoints and matching it with the 2D feature in the target view. On the other hand, Gen6D [58] breaks down the process into three steps. 1). **Detection:** the feature maps of support and target views are extracted using a VGG network [86]. Then, a detected box is obtained by convolving the feature maps, and a parallel branch predicts the box scale. 2). **View Selection:** using the detected box, a view transformer estimates similarity scores

and initial in-plane rotations to find the best-matched support view. 3). **Pose Refinement:** a pose refiner will start from the pose of selected support view and iteratively adjust the 6DoF poses  $\mathbf{p} = [\mathbf{q}, \mathbf{t}, s]$  (parameterized by unit quaternion  $\mathbf{q} = [w, x, y, z]$ , 3D translation vector  $\mathbf{t} = [t_x, t_y, t_z]$ , and scale factor  $s$ ) by estimating an update offset from a  $32^3$  volume built by unprojecting the 2D features.

Although a few generalizable 6DoF estimators [92, 34, 58] have been investigated in the literature, they are known to be vulnerable in extreme sparse view settings, as the sparse point reconstruction may fail [92, 34], or the initial pose may be far from the ground truth due to false positive detections [58] (see Figure 1). Furthermore, Gen6D [58] suffers from GPU memory issue that limit its method to low feature and voxel resolutions ( $32^2$  and  $32^3$ , respectively). On the other hand, OnePose series [92, 34] requires an additional YOLO detector, which may limit its deployment for out-of-distribution objects. To overcome the challenges posed by sparse view settings, we propose three improvements upon the three stages in the pipeline of Gen6D, respectively: robust object detection, parallel pose initialization, and cascade feature volume pose refinement. These tailored designs for few-view settings altogether significantly improve accuracy and robustness in the extremely sparse view scenarios.

### 3.2. Cascade Refinement using Feature Pyramid

Among the three stages, pose refinement plays a crucial role in accurate pose regression. Overall, the iteratively refined general 6DoF pose estimation can be formulated as an optimization problem toward the objective below:

$$\mathcal{L}(\mathbf{p}) = \sum_{i=1}^{N_s} \ell(\mathcal{W}(\mathbf{I}^{(i)} | \mathbf{p}^{(i)}, \mathbf{p}), \mathbf{I}), \quad (1)$$

where  $\mathcal{W}$  wraps the  $i_{th}$  support(reference) images  $\mathbf{I}^{(i)}$  into the tentative target pose  $\mathbf{p}$ , by using the  $i_{th}$  support(reference) pose  $\mathbf{p}^{(i)}$ .  $\ell$  computes a general matching loss over two frames. Both  $\mathcal{W}$  and  $\ell$  can be applied to either key points or whole images [91]. To optimize variable  $\mathbf{p}$ , gradient-based methods are typically adopted, e.g., we can iterative descent the error  $\mathcal{L}$  by  $\mathbf{p}_{t+1} = \mathbf{p}_t - \eta \nabla \mathcal{L}(\mathbf{p}_t)$ . However, since pose estimation faces severe ambiguity, it is intractable to consider a general closed-form  $\mathcal{W}$  and  $\ell$ . Also, the resultant Eq. 1 is highly non-convex, which causes the optimization prone to terminate at a saddle but inaccurate point. The seminal work Gen6D [58] proposes to surrogate the gradient term with a data-driven trained neural network  $s_\theta$ , which directly predicts the update in the pose space:

$$\mathbf{p}_{t+1} = \mathbf{p}_t - \eta s_\theta \left( \mathbf{p}_t \mid \mathbf{I}, \left\{ \mathbf{I}^{(i)}, \mathbf{p}^{(i)} \right\}_{i=1}^{N_s} \right). \quad (2)$$

We note that the learned  $s_\theta$  involves the implicit modeling of both  $\ell$  and  $\mathcal{W}$ , which is more flexible and adaptive to real-world scenarios without handcrafted bias. As illustrated in Eq. 2, the neural network needs to aggregate support view images and evaluate the matching score with the pose at the current iteration. Below we introduce our architectural design for  $s_\theta$  to improve its robustness under few-view setting.

We first obtain the detected object box in the full picture and select its initialized pose  $\mathbf{p}_0$  (also known as the pose in the nearest support view). With the proper initialization, the pose refiner  $s_\theta$  should estimate the update according to the current pose and reference images. To implement the pose refiner, we create a volume within the unit cube at the origin with  $32^3$  vertices. The volume features are derived from two sources: 1) the unprojected feature of the six nearest support images, and 2) the unprojected feature with initial poses and the object in the target view, with mean and variance computed across all support views. The constructed volume will then pass through a 3D ConvNet to be mapped to an update vector in the pose space.

In Gen6D [58], only a single-scale volume is constructed. While a lower-grained volume tentatively mitigates a large pose gap, a finer-grained volume carries more details and improves estimation accuracy. Therefore, the single-scale volume is not optimal under the sparse view setting. As discussed before, the pose refiner predicts a gradient to minimize the matching score between target and support views on the volume space [58]. However, the matching procedure is sensitive to fine details especially when observations are limited, likely to overfit to the high-frequency noises [60, 85]. To conquer these challenges, we propose a cascade volume feature formulation and adopt a coarse-to-fine prediction approach. The rationale is that we start from a coarse-grained volume, which provided low-frequency and contour information to align the rough orientation and position, then we gradually increase the granularity to inject high-frequency signals, which fine-tunes the pose locally to match the low-level details.

**Feature Pyramid Volume Construction.** To strike a balance between volume resolution and computational efficiency, prior work [58], constructed a volume with  $32^3$  vertices, each containing 128 feature dimensions. However, such a single-scale (top-level) feature representation and  $32^3$  volume spatial resolution are not able to accurately regress poses. In contrast, we leverage the Feature Pyramid Network [54] and utilize its feature maps with progressively increased spatial resolutions to construct feature volumes of higher resolutions. Specifically, we construct a three-stage volume with spatial resolutions of  $\{16^3, 32^3, 64^3\}$  by extracting feature maps  $\{P2, P3, P4\}$ . The feature dimensions of these volumes, obtained through the process of unprojecting from FPN, are  $\{64, 32, 16\}$ .



Type	Method	Object Name							Avg.	
		cat	duck	bvise	cam	driller	lamp	eggbox*		glue*
<b>ADD(S)-0.1d</b>										
16-shot	CDPN [51]	0.00	1.20	0.00	0.10	0.66	0.25	0.00	4.25	0.81
	EPro-PNP[14]	0.10	0.00	0.00	0.10	0.79	0.38	0.00	5.21	0.82
	Gen6D [58]	<u>23.55</u>	<u>15.96</u>	41.76	<u>28.30</u>	35.67	60.74	<u>92.39</u>	<u>58.60</u>	<u>44.62</u>
	OnePose++ [34]	20.00	5.07	<b>57.61</b>	23.43	<b>50.80</b>	63.60	81.40	28.50	41.30
	Ours	<b>27.85</b>	<b>19.25</b>	<u>45.83</u>	<b>29.7</b>	<u>39.54</u>	<b>63.84</b>	<b>93.95</b>	<b>62.64</b>	<b>47.83</b>
32-shot	CDPN [51]	2.69	2.54	17.17	5.88	7.14	11.92	11.97	7.01	8.29
	EPro-PNP[14]	1.80	1.50	21.24	6.27	15.06	12.09	19.81	10.71	11.06
	Gen6D [58]	<u>44.81</u>	<u>32.39</u>	62.30	51.56	56.10	81.76	<b>98.21</b>	<b>76.64</b>	<u>62.97</u>
	OnePose++ [34]	35.42	24.31	<b>72.55</b>	<b>71.07</b>	<b>71.55</b>	<b>85.31</b>	95.68	32.91	61.10
	Ours	<b>48.55</b>	<b>40.66</b>	<u>65.98</u>	<u>52.68</u>	<u>61.64</u>	<u>82.53</u>	<b>98.21</b>	<b>76.64</b>	<b>65.86</b>
Full-shot	CDPN [51]	<u>86.63</u>	<u>75.21</u>	<b>98.74</b>	<u>92.84</u>	<u>95.14</u>	97.79	99.62	<b>99.61</b>	<u>93.20</u>
	EPro-PNP[14]	<b>90.52</b>	<b>80.09</b>	96.41	<b>92.94</b>	<b>95.94</b>	<b>99.04</b>	<b>99.91</b>	<u>98.17</u>	<b>94.13</b>
	Gen6D [58]	60.38	40.28	77.13	66.07	67.09	89.80	98.31	87.83	73.30
	OnePose++ [34]	70.40	42.30	<u>97.30</u>	88.00	92.50	<u>97.80</u>	<u>99.70</u>	48.00	79.50
	Ours	60.58	51.27	86.72	70.10	84.84	93.38	98.78	88.51	79.27
<b>Prj-5</b>										
16-shot	CDPN [51]	1.20	5.88	0.00	0.00	2.00	1.25	1.50	1.25	1.63
	EPro-PNP[14]	1.30	1.88	0.97	2.65	3.07	1.63	1.50	2.61	1.95
	Gen6D [58]	<u>68.46</u>	<u>61.12</u>	41.08	<u>46.40</u>	31.70	49.90	<u>88.07</u>	<u>77.4</u>	<u>58.03</u>
	OnePose++ [34]	37.25	14.93	<b>62.17</b>	37.25	<b>58.57</b>	<b>72.93</b>	49.76	24.40	44.66
	Ours	<b>76.45</b>	<b>75.49</b>	<u>46.28</u>	<b>57.23</b>	<u>48.40</u>	<u>53.67</u>	<b>90.07</b>	<b>82.59</b>	<b>66.27</b>
32-shot	CDPN [51]	12.08	47.70	14.94	13.43	4.32	3.24	7.32	11.20	14.28
	EPro-PNP[14]	11.18	38.31	19.59	15.39	9.91	5.85	14.46	16.70	16.42
	Gen6D [58]	<u>92.71</u>	<u>76.61</u>	67.83	84.11	63.13	80.42	<b>95.96</b>	<u>93.91</u>	<u>81.84</u>
	OnePose++ [34]	83.63	69.95	<b>81.37</b>	<b>94.40</b>	<b>72.94</b>	<b>90.59</b>	89.10	30.41	76.50
	Ours	<b>94.01</b>	<b>92.39</b>	<u>69.79</u>	<u>85.03</u>	<u>69.17</u>	<u>84.64</u>	<u>95.58</u>	<b>95.24</b>	<b>85.70</b>
Full-shot	CDPN [51]	<u>99.30</u>	<u>98.40</u>	<u>98.74</u>	98.74	94.85	95.68	<u>99.06</u>	98.36	<u>97.89</u>
	EPro-PNP[14]	<b>99.80</b>	<b>99.06</b>	98.64	<u>99.12</u>	<b>97.32</b>	<u>97.02</u>	<b>99.25</b>	<b>98.94</b>	<b>98.64</b>
	Gen6D [58]	96.10	79.71	82.46	90.78	72.44	91.60	97.84	96.23	88.40
	OnePose++ [34]	98.70	97.70	<b>99.60</b>	<b>99.60</b>	93.10	<b>98.80</b>	98.70	51.80	94.25
	Ours	99.00	93.50	93.41	96.27	<u>94.95</u>	96.93	98.31	<u>98.84</u>	96.40

Table 1. **Quantitative Comparison on LINEMOD Dataset.** The table shows the performance comparison of Cas6D with several generalizable methods in both sparse view and full-shot settings. The best and second-best performing methods are highlighted in bold and underlined, respectively. Cas6D outperforms previous generalizable (model-free) methods consistently in all settings.

**Pose Hypothesis Range in Each Stage** To improve the accuracy of initial pose estimation using the volume feature, there are two approaches: manually setting the sampling range  $\mathcal{R}_t$  at each stage  $t$ , or caching the distance between predictions and ground truth over the entire training set. Subsequently, the sampling range can be gradually reduced in each stage by a scaling factor  $w_t$ , such that  $\mathcal{R}_{t+1} = w_t \times \mathcal{R}_t$ . In our implementation, we choose  $w_t < 1$  to progressively narrow down the pose search range.

**Camera Pose Parameterization** To refine the estimated 6DoF pose  $p_t$  in the  $t$ -th stage, we can perform direct regression of the residual using the Mean Squared Error (MSE) loss. However, under sparse view scenarios, where there is a large gap between initializations and ground truth, this approach may lead to unstable learning. To address this issue, we discretize the measured pose range into a set of discrete bins and use classification loss for pose bin estimation. We denote each interval of adjacent bins as  $I_i$  in stage  $i$ . The pose estimation task then becomes a classification problem of assigning the correct viewspace bin to the initial poses. In the later stages, we apply finer pose intervals to

recover more detailed poses:  $I_{t+1} = v_t \times I_t$ , where  $v_t < 1$  narrows the bin interval gradually.

### 3.3. Parallel Pose Initialization

In the case of sparse input, performance is significantly affected by the inaccurate pose initialization when searching for the closest support images. Previous work, such as FS6D, assumes that accurate depth maps are available for all captures. However, depth maps are not always available for everyday objects. To mitigate the degradation of performance in the sparse-view setting, we propose an initialization scheme that generates multiple pose hypotheses based on the top-K similarity scores between the target view and all support views. With this initialization scheme, the refiner can obtain a better starting point by warping the support to the target feature volumes, as some of the hypotheses may be relatively close to the ground truth.

### 3.4. Detection with Self-supervised Semantic Correspondence.

One of the most common failure modes in 6DoF estimation is the inability of the network to find feature correspondences between different views of the same object, which can be caused by noisy backgrounds or low-textured objects. This problem is further amplified in the few-shot setting where fewer observations are available. To address this issue, we draw inspiration from the 2D co-segmentation work [4] which demonstrates that DINO, a powerful feature extractor, can learn feature correspondences for image pairs. Therefore, we incorporate the frozen DINO-ViT [12] feature to aid the detector in localizing the correct object box. The adoption of the frozen DINO feature incurs only negligible memory cost, which will be discussed in the experiment section.

### 3.5. Loss Function

The three modules are trained independently with their own losses. We describe the loss function of the cascade refiner as follows and state other losses in the supplementary due to space limitation. We first transform the quaternion representation to rotation matrix and translation vector, sample  $v_i^3$  voxel points in each stage of the object coordinate system ( $v_i$  is voxel resolution), and transform them into camera coordinate system using object poses. We calculate the distance of the transformed points by using predicted and the ground-truth poses.

$$\ell_{pose} = \sum_{k=1}^N \lambda_k \cdot \sum_{m=1}^{v_k^3} \|\mathcal{T}_{pr}(p_k | k, m) - \mathcal{T}_{gt}(p_k | k, m)\|_2 \quad (3)$$

where  $k$  means refine stage index,  $m$  is voxel index,  $\lambda_k$  indicate loss weights of each stage, and  $\mathcal{T}_{pr}(p_k | k, m)$  and  $\mathcal{T}_{gt}(p_k | k, m)$  indicate the transformed points, respectively.

## 4. Experiment

### 4.1. Experiment Setup

**LINEMOD Dataset [37].** The LINEMOD dataset is a widely used dataset for object pose estimation. It includes 13 videos, each featuring 13 low-textured objects, and approximately 1000 test images for each object, which are used as target images for evaluation.

**GenMOP Dataset [58].** The GenMOP dataset [58] comprises 10 objects captured in two video sequences under varying environmental conditions, such as different backgrounds and lighting conditions. Each video sequence is composed of approximately 200 images.

**Training Details** We conducted experiments with other generalizable methods [58] using the same training datasets, which include 2000 ShapeNet models [13], 1023 objects from the Google Scanned Object dataset [99], 5 objects

from the GenMOP dataset [58], and 5 objects from the LINEMOD dataset [37]. To evaluate the sparse-view scenario, we randomly selected 16 to 64 views for training the refiner of our method and Gen6D [58]. We select the top-3 pose candidates as initialization and evaluate the comparisons using Cas6D with 3-stage with volume feature size as  $(16^2 \times 64, 32^2 \times 32, 64^2 \times 16)$ . We cache and update the maximum pose difference to determine the range. Throughout all stages, we set annealing factors  $v_i$  and  $w_i$  to 0.5, pose bin number as  $\{16, 8, 4\}$  for all components in 6DoF poses  $p$ . We use the same data pre-processing and training recipe as Gen6D [58]. We select the sparse views from all evaluation views for evaluation using farthest point sampling (FPS) [58]. All experiments were performed using 8 Tesla V100 GPUs with 32GB memory.

**Metrics** We adopted the commonly used *Average Distance(ADD)* and *Projection Error* as metrics to evaluate the performance of all methods. For an object  $\mathcal{O}$  composed of vertices  $v$ , the ADD/ADDS for both asymmetric and symmetric objects with the predicted pose  $\mathbf{R}, \mathbf{t}$  and ground truth pose  $\mathbf{R}^*, \mathbf{t}^*$  were calculated using the following formulas:

$$ADD = \frac{1}{m} \sum_{v \in \mathcal{O}} \|(\mathbf{R}v + \mathbf{t}) - (\mathbf{R}^*v + \mathbf{t}^*)\| \quad (4)$$

$$ADDS = \frac{1}{m} \sum_{v_1 \in \mathcal{O}} \min_{v_2 \in \mathcal{O}} \|(\mathbf{R}v_1 + \mathbf{t}) - (\mathbf{R}^*v_2 + \mathbf{t}^*)\| \quad (5)$$

We computed the recall rate on the ADD and ADDS metrics with 10% of the object diameter (ADD-0.1d and ADDS-0.1d). For the projection error, we computed the recall rate at 5 pixels and referred to it as Prj-5.

### 4.2. Comparisons

We compared the proposed Cas6D with two categories of baselines. The first category is generalizable methods [58, 34] with the same training datasets as ours. All objects for evaluation are not seen in the training sets. Note that, OnePose++ [34] leverage an additional YOLOv5<sup>1</sup> as object detector. The second category is instance-level methods [51, 14] that require CAD models and are separately trained for each object in the test set.

**Results on LINEMOD** We compare the proposed method with other state-of-the-art methods under  $\{16, 32, \text{full}(\text{all support})\}$  views settings. Specifically, we re-trained the refiner of the original Gen6D [58] model, which randomly selects from 16 to 64 support views to find the nearest support to align with our training recipe. As is shown in Table 1, Cas6D consistently outperforms other generalizable baselines under all settings. Under the full-shot setting, instance-level methods perform with almost 100%

<sup>1</sup><https://github.com/ultralytics/yolov5>

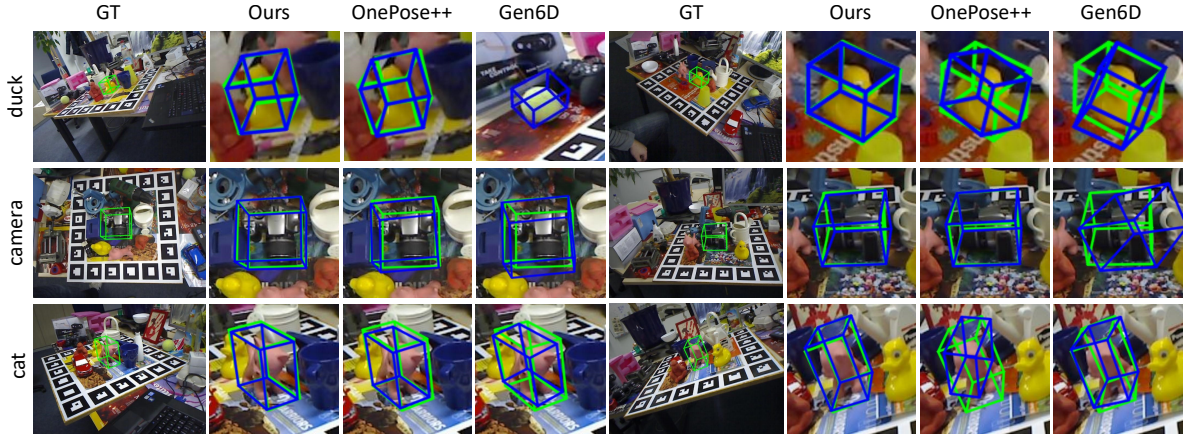


Figure 3. **Qualitative results on the LINEMOD dataset under 32-shot setting.** The ground-truth poses are drawn in green while estimated poses are drawn in blue. Gen6D [58] may erroneously detect the incorrect object with a similar appearance, while Cas6D is more robust against appearance noises. Further, Cas6D usually generates a more tight 3D orientated box than other methods, owing to the coarse-to-fine refinement by using 2D feature pyramid.

Type	Method	Object Name					Avg.
		Chair	PlugEN	Piggy	Scissors	TFormer	
ADD(S)-0.1d							
16-shot	Gen6D	48.50	10.54	59.80	24.57	26.59	34.00
	OnePose++	25.00	1.87	47.24	25.43	21.42	24.19
	Ours	<b>52.87</b>	<b>12.58</b>	<b>64.09</b>	<b>26.80</b>	<b>28.74</b>	<b>37.01</b>
32-shot	Gen6D	51.50	11.68	65.32	32.75	44.0	41.05
	OnePose++	31.0	4.67	70.85	36.64	26.19	33.87
	Ours	<b>54.85</b>	<b>15.45</b>	<b>67.94</b>	<b>35.17</b>	<b>46.61</b>	<b>44.00</b>
Full-shot	Gen6D	61.50	19.63	74.37	33.62	63.89	50.60
	OnePose++	58.50	4.67	94.47	39.22	59.13	51.20
	Ours	<b>64.00</b>	<b>23.36</b>	<b>77.87</b>	<b>36.88</b>	<b>65.47</b>	<b>53.52</b>
Prj-5							
16-shot	Gen6D	33.50	66.43	90.45	79.31	90.87	72.11
	OnePose++	<b>40.00</b>	11.21	19.6	44.83	63.10	35.75
	Ours	39.58	<b>73.11</b>	<b>95.49</b>	<b>84.74</b>	<b>93.50</b>	<b>77.28</b>
32-shot	Gen6D	42.50	68.69	94.98	87.06	91.50	76.95
	OnePose++	<b>49.50</b>	14.48	56.28	70.26	79.36	53.98
	Ours	46.71	<b>86.41</b>	<b>99.60</b>	<b>90.83</b>	<b>99.50</b>	<b>84.61</b>
Full-shot	Gen6D	46.71	70.41	98.60	96.83	96.37	81.78
	OnePose++	<b>81.00</b>	75.23	95.98	82.75	90.48	85.09
	Ours	62.50	<b>78.67</b>	<b>99.50</b>	<b>97.43</b>	<b>99.50</b>	<b>87.52</b>

Table 2. **Quantitative results on GenMOP dataset.** We report the comparisons with several generalizable (CAD model-free) methods, under sparse view settings and full-shot settings.

accuracy owing to their use of ground-truth CAD models. The performance difference between our proposed method and OnePose++[34] can be attributed to the latter’s inability to reconstruct an accurate point cloud when the number of available support views decreases, making it difficult to find the best matches. Figure 3 illustrates the qualitative results, where it can be observed that Gen6D fails to detect the correct object box, leading to an incorrect pose regression result (4th column). In contrast, our Cas6D is more robust under the sparse-view setting, enabling it to detect the object pose accurately and estimate the final object pose.

**Results on GenMOP** We evaluate the generalization ability of our proposed framework on the GenMOP dataset [58] and use the same evaluation criterion as that

of the LINEMOD dataset. Table 1 presents the comparison results, and we find that Cas6D outperforms the compared baselines under sparse-view settings. Furthermore, the visualized pose estimations on various objects in Figure 4 further validate the effectiveness of our method, which can be attributed to the robust object detection, parallel pose initialization, and cascade pose refinement with feature pyramid.

### 4.3. Ablation Studies

We conduct ablation studies on the LINEMOD test set [37] to verify the effectiveness of the proposed design. The results are presented in Table 3.

**Volume Construction with Feature Pyramids** In order to demonstrate the advantage of volume feature construction using feature pyramids, we compare our approach with single-scale construction [58] in this ablation study. We replace the single scale feature in Gen6D [58] (Table 3, ID 1) with our feature pyramids (Table 3, ID 2) while keeping the single-scale volume feature size fixed at  $32^3 \times 128$ . We found that using feature pyramids led to an improvement in averaged ADD-0.1d/Prj-5 from 63.0/81.8 to 63.2/82.15, with negligible GPU memory overheads. This validates that fusing multi-scale features enriches the volume representation and leads to better results.

**How Many Cascade Stages Should be Used?** We conduct experiments with different cascade stage numbers (2, 3) and report the corresponding results in Table 3 (ID 4 and 5). We only use one pose candidate as the input of the cascade refiner for this comparison. The volume feature is constructed using FPN feature maps from three spatial levels ( $16^2$ ,  $32^2$ ,  $64^2$ ) with volume sizes of ( $16^2 \times 64$ ,  $32^2 \times 32$ ,  $64^2 \times 16$ ). Our results show that as the number of stages increases, the performance first improves and then stabilizes.

**The Effect of Coarse-to-fine framework** Our coarse-to-fine framework with a *novel pose parameterization*



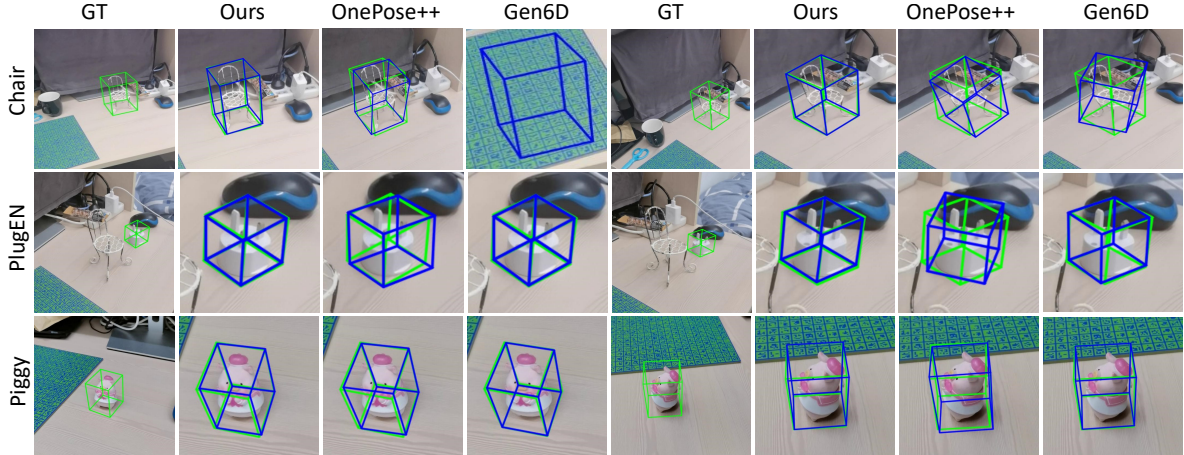


Figure 4. **Qualitative results on the GenMOP dataset [58] under 32-shot setting.** The ground-truth poses are drawn in green while estimated poses are drawn in blue. Cas6D performs consistently better than other baselines, by utilizing the robust object detection, multiple-pose initialization and coarse-to-fine pose refinement.

ID	DINO Feat.?	Feature Pyramid?	Init. Pose Num.	Stage Num.	Reg./Cls.?	Avg. ADD-0.1d	Avg. Prj-5	GPU Mem.
1	✗	✗	1	1	Reg	63.00	81.80	826M
2	✗	✓	1	1	Reg	63.20	82.15	846M
3	✓	✓	1	1	Reg	63.80	82.90	886M
4	✓	✓	1	2	Cls	65.20	84.00	695M
5	✓	✓	1	3	Cls	65.50	84.80	789M
6	✓	✓	3	3	Cls	65.86	85.70	805M
7	✓	✓	3	3	Reg	63.68	83.29	805M
8	✓	✓	5	3	Cls	65.28	84.83	815M
9	✓	✓	7	3	Cls	63.69	81.43	835M

Table 3. **Ablation Studies.** We perform extensive experiments to validate our proposed designs, by reporting the pose estimation accuracy, and GPU memory consumption at the inference stage. Results are averaged on LINEMOD [37] dataset under the 32-shot setting.

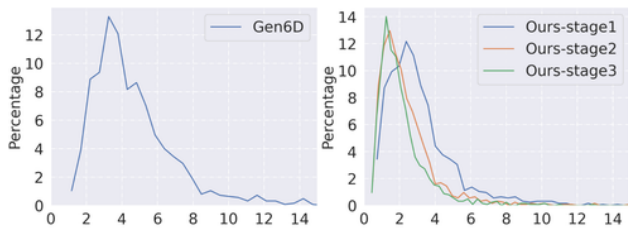


Figure 5. **Averaged Pose Residual:** We show the percentage (y-axis) and the pose error from GT (x-axis).

and *adaptive pose sampling* addresses the limitation of a regression-based single-scale pose volume feature (Figure 5, left), enabling a wider pose search range and fine-grained predictions (Figure 5, right).

**Impact of Parallel Pose Initialization** The use of multiple parallel pose initializations from the similarity network helps the refiner to find the support view with the lowest feature warping error. To test this, we designed experiments where we used the top {1, 3, 5, 7} pose initializations with the highest similarity score. Table 3 shows the results in IDs 5, 6, 8, and 9. The accuracy increases when more potential support views are included, but when more than 5 views are

	cat	duck	bvise	cam	driller	Avg.
Gen6D	76.99	42.15	63.33	72.92	48.78	60.83
Cas6D(Ours)	79.46	67.44	66.32	76.39	59.35	69.70

Table 4. **Box Detection Accuracy.** We evaluated the object detection accuracy on the LINEMOD dataset under the 32-shot setting. Cas6D outperforms Gen6D in terms of  $mAP@.5:.95$  (%) on the test set, demonstrating that the self-supervised feature representation benefits correspondence matching across object views.

used, the performance starts to degrade because these pose candidates may be too far from the target view.

**Shall We use Regress or Discrete Pose Bins?** We conducted a comparison between regression and classification-based pose residual estimation methods under sparse view settings. As shown in ID 6 and 7 of Table 3, we observe that our method performed better when mapping the gap (from initial to GT) to discrete pose bins, achieving 85.70 on Prj-5, compared to 83.29 achieved by the regression-based method. This indicates that using discrete pose bins is more effective in sparse view scenarios.

**The Effect of Pre-trained ViTs** The effectiveness of self-supervised trained representation has been demonstrated in 2D co-segmentation [4]. In this work, we demonstrate the



importance of pre-training for feature learning in the entire 6DoF pipeline for object detection. The average ADD-0.1d/Prj-5 improves from 63.2/82.15 to 63.80/82.90 with negligible impact on GPU memory overheads (IDs 2 and 3 of Table 3). We also evaluate the mAP@.5:.95 (%) of the detected box against the ground truth and observe an improvement from 60.83 to 69.70, as presented in Table 4.

## 5. Conclusion, Limitations and Future Works

In this paper, we propose a cascade 6DoF pose estimation framework, called **Cas6D**, for few-shot object pose estimation with multi-view RGB images. Our approach leverages self-supervised pre-trained DINO-ViT representations and a divide-and-conquer model design to formulate a robust arbitrary object detector. We use top-K similar support views to initialize multiple pose candidates and design a cascade volume feature formulation to generate finer poses with finer volume features, narrowing the pose search range at each stage using multi-scale FPN features. Our framework outperforms all other generalizable baselines under both few-shot and full-shot settings while reducing inference memory requirements. However, the current implementation of our framework requires constructing 3D volumes and performing 3D convolutional layers for pose regression, limiting its application to ultra-high resolution scenarios. We plan to explore more efficient implementations of volume feature aggregation.

## References

- [1] Idan Achituve, Haggai Maron, and Gal Chechik. Self-supervised learning for domain adaptation on point clouds. In *Proceedings of the IEEE/CVF winter conference on applications of computer vision*, pages 123–133, 2021. 3
- [2] Panos Achlioptas, Olga Diamanti, Ioannis Mitliagkas, and Leonidas Guibas. Learning representations and generative models for 3d point clouds. In *International conference on machine learning*, pages 40–49. PMLR, 2018. 3
- [3] Adel Ahmadyan, Liangkai Zhang, Artsiom Ablavatski, Jianing Wei, and Matthias Grundmann. Objectron: A large scale dataset of object-centric videos in the wild with pose annotations. In *Proceedings of the IEEE/CVF conference on computer vision and pattern recognition*, pages 7822–7831, 2021. 1
- [4] Shir Amir, Yossi Gandelsman, Shai Bagon, and Tali Dekel. Deep vit features as dense visual descriptors. *arXiv preprint arXiv:2112.05814*, 2(3):4, 2021. 2, 6, 8
- [5] Xuyang Bai, Zixin Luo, Lei Zhou, Hongbo Fu, Long Quan, and Chiew-Lan Tai. D3feat: Joint learning of dense detection and description of 3d local features. In *Proceedings of the IEEE/CVF conference on computer vision and pattern recognition*, pages 6359–6367, 2020. 3
- [6] Vassileios Balntas, Andreas Doulamoglou, Caner Sahin, Juil Sock, Rigas Kouskouridas, and Tae-Kyun Kim. Pose guided rgb-d feature learning for 3d object pose estimation. In *Proceedings of the IEEE international conference on computer vision*, pages 3856–3864, 2017. 3
- [7] Jonathan T Barron, Ben Mildenhall, Matthew Tancik, Peter Hedman, Ricardo Martin-Brualla, and Pratul P Srinivasan. Mip-nerf: A multiscale representation for anti-aliasing neural radiance fields. In *IEEE International Conference on Computer Vision (ICCV)*, 2021. 3
- [8] Piotr Bojanowski and Armand Joulin. Unsupervised learning by predicting noise. In *International Conference on Machine Learning*, pages 517–526. PMLR, 2017. 3
- [9] Benjamin Busam, Hyun Jun Jung, and Nassir Navab. I like to move it: 6d pose estimation as an action decision process. *arXiv preprint arXiv:2009.12678*, 2020. 3
- [10] Chenjie Cao, Xinlin Ren, and Yanwei Fu. Mvsformer: Learning robust image representations via transformers and temperature-based depth for multi-view stereo. *arXiv preprint arXiv:2208.02541*, 2022. 3
- [11] Mathilde Caron, Piotr Bojanowski, Armand Joulin, and Matthijs Douze. Deep clustering for unsupervised learning of visual features. In *Proceedings of the European conference on computer vision (ECCV)*, pages 132–149, 2018. 3
- [12] Mathilde Caron, Hugo Touvron, Ishan Misra, Hervé Jégou, Julien Mairal, Piotr Bojanowski, and Armand Joulin. Emerging properties in self-supervised vision transformers. In *Proceedings of the IEEE/CVF International Conference on Computer Vision*, pages 9650–9660, 2021. 2, 3, 6
- [13] Angel X Chang, Thomas Funkhouser, Leonidas Guibas, Pat Hanrahan, Qixing Huang, Zimo Li, Silvio Savarese, Manolis Savva, Shuran Song, Hao Su, et al. Shapenet: An information-rich 3d model repository. *arXiv preprint arXiv:1512.03012*, 2015. 6
- [14] Hansheng Chen, Pichao Wang, Fan Wang, Wei Tian, Lu Xiong, and Hao Li. Epro-ntp: Generalized end-to-end probabilistic perspective-n-points for monocular object pose estimation. In *Proceedings of the IEEE/CVF Conference on Computer Vision and Pattern Recognition*, pages 2781–2790, 2022. 5, 6
- [15] Rui Chen, Songfang Han, Jing Xu, and Hao Su. Point-based multi-view stereo network. In *Proceedings of the IEEE/CVF international conference on computer vision*, pages 1538–1547, 2019. 3
- [16] Wei Chen, Xi Jia, Hyung Jin Chang, Jinming Duan, Linlin Shen, and Ales Leonardis. Fs-net: Fast shape-based network for category-level 6d object pose estimation with decoupled rotation mechanism. In *Proceedings of the IEEE/CVF Conference on Computer Vision and Pattern Recognition*, pages 1581–1590, 2021. 2
- [17] Xu Chen, Zijian Dong, Jie Song, Andreas Geiger, and Otmar Hilliges. Category level object pose estimation via neural analysis-by-synthesis. In *Computer Vision—ECCV 2020: 16th European Conference, Glasgow, UK, August 23–28, 2020, Proceedings, Part XXVI 16*, pages 139–156. Springer, 2020. 1, 2
- [18] Shuo Cheng, Zexiang Xu, Shilin Zhu, Zhuwen Li, Li Erran Li, Ravi Ramamoorthi, and Hao Su. Deep stereo using adaptive thin volume representation with uncertainty awareness. In *Proceedings of the IEEE/CVF Conference*

- on *Computer Vision and Pattern Recognition*, pages 2524–2534, 2020. [3](#)
- [19] Christopher Choy, Jaesik Park, and Vladlen Koltun. Fully convolutional geometric features. In *Proceedings of the IEEE/CVF international conference on computer vision*, pages 8958–8966, 2019. [3](#)
- [20] Meghal Dani, Karan Narain, and Ramya Hebbalaguppe. 3dposelite: a compact 3d pose estimation using node embeddings. In *Proceedings of the IEEE/CVF Winter Conference on Applications of Computer Vision*, pages 1878–1887, 2021. [3](#)
- [21] Haowen Deng, Tolga Birdal, and Slobodan Ilic. Ppfnets: Global context aware local features for robust 3d point matching. In *Proceedings of the IEEE conference on computer vision and pattern recognition*, pages 195–205, 2018. [3](#)
- [22] Xinke Deng, Junyi Geng, Timothy Bretl, Yu Xiang, and Dieter Fox. icaps: Iterative category-level object pose and shape estimation. *IEEE Robotics and Automation Letters*, 7(2):1784–1791, 2022. [2](#)
- [23] Yan Di, Fabian Manhardt, Gu Wang, Xiangyang Ji, Nassir Navab, and Federico Tombari. So-pose: Exploiting self-occlusion for direct 6d pose estimation. In *Proceedings of the IEEE/CVF International Conference on Computer Vision*, pages 12396–12405, 2021. [2](#)
- [24] Yan Di, Ruida Zhang, Zhiqiang Lou, Fabian Manhardt, Xiangyang Ji, Nassir Navab, and Federico Tombari. Gvp-pose: Category-level object pose estimation via geometry-guided point-wise voting. In *Proceedings of the IEEE/CVF Conference on Computer Vision and Pattern Recognition*, pages 6781–6791, 2022. [2](#)
- [25] Carl Doersch, Abhinav Gupta, and Alexei A Efros. Unsupervised visual representation learning by context prediction. In *Proceedings of the IEEE international conference on computer vision*, pages 1422–1430, 2015. [3](#)
- [26] Chelsea Finn, Pieter Abbeel, and Sergey Levine. Model-agnostic meta-learning for fast adaptation of deep networks. In *International conference on machine learning*, pages 1126–1135. PMLR, 2017. [3](#)
- [27] Matheus Gadelha, Rui Wang, and Subhansu Maji. Multiresolution tree networks for 3d point cloud processing. In *Proceedings of the European Conference on Computer Vision (ECCV)*, pages 103–118, 2018. [3](#)
- [28] Victor Garcia and Joan Bruna. Few-shot learning with graph neural networks. *arXiv preprint arXiv:1711.04043*, 2017. [3](#)
- [29] Zan Gojcic, Caifa Zhou, Jan D Wegner, and Andreas Wieser. The perfect match: 3d point cloud matching with smoothed densities. In *Proceedings of the IEEE/CVF conference on computer vision and pattern recognition*, pages 5545–5554, 2019. [3](#)
- [30] Walter Goodwin, Sagar Vaze, Ioannis Havoutis, and Ingmar Posner. Zero-shot category-level object pose estimation. In *Computer Vision–ECCV 2022: 17th European Conference, Tel Aviv, Israel, October 23–27, 2022, Proceedings, Part XXXIX*, pages 516–532. Springer, 2022. [2](#)
- [31] Thibault Groueix, Matthew Fisher, Vladimir G Kim, Bryan C Russell, and Mathieu Aubry. A papier-mâché approach to learning 3d surface generation. In *Proceedings of the IEEE conference on computer vision and pattern recognition*, pages 216–224, 2018. [3](#)
- [32] Xiaodong Gu, Zhiwen Fan, Siyu Zhu, Zuozhuo Dai, Feitong Tan, and Ping Tan. Cascade cost volume for high-resolution multi-view stereo and stereo matching. In *IEEE Conference on Computer Vision and Pattern Recognition (CVPR)*, 2020. [3](#)
- [33] Kaveh Hassani and Mike Haley. Unsupervised multi-task feature learning on point clouds. In *Proceedings of the IEEE/CVF International Conference on Computer Vision*, pages 8160–8171, 2019. [3](#)
- [34] Xingyi He, Jiaming Sun, Yuang Wang, Di Huang, Hujun Bao, and Xiaowei Zhou. Onepose++: Keypoint-free one-shot object pose estimation without cad models. *arXiv preprint arXiv:2301.07673*, 2023. [1](#), [2](#), [3](#), [4](#), [5](#), [6](#), [7](#)
- [35] Yisheng He, Yao Wang, Haoqiang Fan, Jian Sun, and Qifeng Chen. Fs6d: Few-shot 6d pose estimation of novel objects. In *Proceedings of the IEEE/CVF Conference on Computer Vision and Pattern Recognition*, pages 6814–6824, 2022. [2](#), [3](#)
- [36] Stefan Hinterstoisser, Stefan Holzer, Cedric Cagniart, Slobodan Ilic, Kurt Konolige, Nassir Navab, and Vincent Lepetit. Multimodal templates for real-time detection of texture-less objects in heavily cluttered scenes. In *2011 international conference on computer vision*, pages 858–865. IEEE, 2011. [3](#)
- [37] Stefan Hinterstoisser, Vincent Lepetit, Slobodan Ilic, Stefan Holzer, Gary Bradski, Kurt Konolige, and Nassir Navab. Model based training, detection and pose estimation of texture-less 3d objects in heavily cluttered scenes. In *Computer Vision–ACCV 2012: 11th Asian Conference on Computer Vision, Daejeon, Korea, November 5-9, 2012, Revised Selected Papers, Part I 11*, pages 548–562. Springer, 2013. [2](#), [6](#), [7](#), [8](#)
- [38] Stefan Hinterstoisser, Vincent Lepetit, Naresh Rajkumar, and Kurt Konolige. Going further with point pair features. In *Computer Vision–ECCV 2016: 14th European Conference, Amsterdam, The Netherlands, October 11-14, 2016, Proceedings, Part III 14*, pages 834–848. Springer, 2016. [3](#)
- [39] Tomas Hodan, Daniel Barath, and Jiri Matas. Epos: Estimating 6d pose of objects with symmetries. In *Proceedings of the IEEE/CVF conference on computer vision and pattern recognition*, pages 11703–11712, 2020. [2](#)
- [40] Tomas Hodan, Frank Michel, Eric Brachmann, Wadim Kehl, Anders GlentBuch, Dirk Kraft, Bertram Drost, Joel Vidal, Stephan Ihrke, Xenophon Zabulis, et al. Bop: Benchmark for 6d object pose estimation. In *Proceedings of the European conference on computer vision (ECCV)*, pages 19–34, 2018. [2](#)
- [41] Tomáš Hodaň, Martin Sundermeyer, Bertram Drost, Yann Labbé, Eric Brachmann, Frank Michel, Carsten Rother, and Jiří Matas. Bop challenge 2020 on 6d object localization. In *Computer Vision–ECCV 2020 Workshops: Glasgow, UK, August 23–28, 2020, Proceedings, Part II 16*, pages 577–594. Springer, 2020. [2](#)

- [42] Yinlin Hu, Pascal Fua, Wei Wang, and Mathieu Salzmann. Single-stage 6d object pose estimation. In *Proceedings of the IEEE/CVF conference on computer vision and pattern recognition*, pages 2930–2939, 2020. 2
- [43] Xu Ji, Joao F Henriques, and Andrea Vedaldi. Invariant information clustering for unsupervised image classification and segmentation. In *Proceedings of the IEEE/CVF International Conference on Computer Vision*, pages 9865–9874, 2019. 3
- [44] Longlong Jing, Yucheng Chen, Ling Zhang, Mingyi He, and Yingli Tian. Self-supervised modal and view invariant feature learning. *arXiv preprint arXiv:2005.14169*, 2020. 3
- [45] Wadim Kehl, Fabian Manhardt, Federico Tombari, Slobodan Ilic, and Nassir Navab. Ssd-6d: Making rgb-based 3d detection and 6d pose estimation great again. In *Proceedings of the IEEE international conference on computer vision*, pages 1521–1529, 2017. 1
- [46] Yann Labbé, Justin Carpentier, Mathieu Aubry, and Josef Sivic. Cosypose: Consistent multi-view multi-object 6d pose estimation. In *Computer Vision–ECCV 2020: 16th European Conference, Glasgow, UK, August 23–28, 2020, Proceedings, Part XVII 16*, pages 574–591. Springer, 2020. 1, 2
- [47] Jiaxin Li, Ben M Chen, and Gim Hee Lee. So-net: Self-organizing network for point cloud analysis. In *Proceedings of the IEEE conference on computer vision and pattern recognition*, pages 9397–9406, 2018. 3
- [48] Jiaxin Li and Gim Hee Lee. Usip: Unsupervised stable interest point detection from 3d point clouds. In *Proceedings of the IEEE/CVF international conference on computer vision*, pages 361–370, 2019. 3
- [49] Xinghui Li, Kai Han, Shuda Li, and Victor Prisacariu. Dual-resolution correspondence networks. *Advances in Neural Information Processing Systems*, 33:17346–17357, 2020. 3
- [50] Yi Li, Gu Wang, Xiangyang Ji, Yu Xiang, and Dieter Fox. Deepim: Deep iterative matching for 6d pose estimation. In *Proceedings of the European Conference on Computer Vision (ECCV)*, pages 683–698, 2018. 3
- [51] Zhigang Li, Gu Wang, and Xiangyang Ji. Cdpn: Coordinates-based disentangled pose network for real-time rgb-based 6-dof object pose estimation. In *Proceedings of the IEEE/CVF International Conference on Computer Vision*, pages 7678–7687, 2019. 1, 5, 6
- [52] Jiehong Lin, Hongyang Li, Ke Chen, Jiangbo Lu, and Kui Jia. Sparse steerable convolutions: An efficient learning of se (3)-equivariant features for estimation and tracking of object poses in 3d space. *Advances in Neural Information Processing Systems*, 34:16779–16790, 2021. 2
- [53] Jiehong Lin, Zewei Wei, Zhihao Li, Songcen Xu, Kui Jia, and Yuanqing Li. Dualposenet: Category-level 6d object pose and size estimation using dual pose network with refined learning of pose consistency. In *Proceedings of the IEEE/CVF International Conference on Computer Vision*, pages 3560–3569, 2021. 2
- [54] Tsung-Yi Lin, Piotr Dollár, Ross Girshick, Kaiming He, Bharath Hariharan, and Serge Belongie. Feature pyramid networks for object detection. In *CVPR*, pages 2117–2125, 2017. 4
- [55] Yunzhi Lin, Thomas Müller, Jonathan Tremblay, Bowen Wen, Stephen Tyree, Alex Evans, Patricio A Vela, and Stan Birchfield. Parallel inversion of neural radiance fields for robust pose estimation. *arXiv preprint arXiv:2210.10108*, 2022. 3
- [56] Ce Liu, Jenny Yuen, and Antonio Torralba. Sift flow: Dense correspondence across scenes and its applications. *IEEE transactions on pattern analysis and machine intelligence*, 33(5):978–994, 2010. 3
- [57] Xingyu Liu, Rico Jonschkowski, Anelia Angelova, and Kurt Konolige. Keypose: Multi-view 3d labeling and key-point estimation for transparent objects. In *Proceedings of the IEEE/CVF conference on computer vision and pattern recognition*, pages 11602–11610, 2020. 2
- [58] Yuan Liu, Yilin Wen, Sida Peng, Cheng Lin, Xiaoxiao Long, Taku Komura, and Wenping Wang. Gen6d: Generalizable model-free 6-dof object pose estimation from rgb images. In *Computer Vision–ECCV 2022: 17th European Conference, Tel Aviv, Israel, October 23–27, 2022, Proceedings, Part XXXII*, pages 298–315. Springer, 2022. 1, 2, 3, 4, 5, 6, 7, 8
- [59] David G Lowe. Object recognition from local scale-invariant features. In *Proceedings of the seventh IEEE international conference on computer vision*, volume 2, pages 1150–1157. Ieee, 1999. 3
- [60] David G Lowe. Distinctive image features from scale-invariant keypoints. *International journal of computer vision*, 60:91–110, 2004. 4
- [61] Zixin Luo, Tianwei Shen, Lei Zhou, Siyu Zhu, Runze Zhang, Yao Yao, Tian Fang, and Long Quan. Geodesc: Learning local descriptors by integrating geometry constraints. In *Proceedings of the European conference on computer vision (ECCV)*, pages 168–183, 2018. 3
- [62] Zixin Luo, Lei Zhou, Xuyang Bai, Hongkai Chen, Jiahui Zhang, Yao Yao, Shiwei Li, Tian Fang, and Long Quan. Aslfeat: Learning local features of accurate shape and localization. In *Proceedings of the IEEE/CVF conference on computer vision and pattern recognition*, pages 6589–6598, 2020. 3
- [63] Jonathan Masci, Ueli Meier, Dan Cireşan, and Jürgen Schmidhuber. Stacked convolutional auto-encoders for hierarchical feature extraction. In *Artificial Neural Networks and Machine Learning–ICANN 2011: 21st International Conference on Artificial Neural Networks, Espoo, Finland, June 14–17, 2011, Proceedings, Part I 21*, pages 52–59. Springer, 2011. 3
- [64] Lars Mescheder, Sebastian Nowozin, and Andreas Geiger. Adversarial variational bayes: Unifying variational autoencoders and generative adversarial networks. In *International conference on machine learning*, pages 2391–2400. PMLR, 2017. 3
- [65] Ben Mildenhall, Pratul P Srinivasan, Matthew Tancik, Jonathan T Barron, Ravi Ramamoorthi, and Ren Ng. Nerf: Representing scenes as neural radiance fields for view synthesis. In *European conference on computer vision*, pages 405–421. Springer, 2020. 3



- [66] Thomas Müller, Alex Evans, Christoph Schied, and Alexander Keller. Instant neural graphics primitives with a multiresolution hash encoding. *ACM Transactions on Graphics (ToG)*, 41(4):1–15, 2022. 3
- [67] Tsendsuren Munkhdalai and Hong Yu. Meta networks. In *International conference on machine learning*, pages 2554–2563. PMLR, 2017. 3
- [68] Michael Niemeyer, Jonathan T Barron, Ben Mildenhall, Mehdi SM Sajjadi, Andreas Geiger, and Noha Radwan. Regnerf: Regularizing neural radiance fields for view synthesis from sparse inputs. In *Proceedings of the IEEE/CVF Conference on Computer Vision and Pattern Recognition*, pages 5480–5490, 2022. 2
- [69] Mehdi Noroozi and Paolo Favaro. Unsupervised learning of visual representations by solving jigsaw puzzles. In *Computer Vision—ECCV 2016: 14th European Conference, Amsterdam, The Netherlands, October 11–14, 2016, Proceedings, Part VI*, pages 69–84. Springer, 2016. 3
- [70] Brian Okorn, Qiao Gu, Martial Hebert, and David Held. Zephyr: Zero-shot pose hypothesis rating. In *2021 IEEE International Conference on Robotics and Automation (ICRA)*, pages 14141–14148. IEEE, 2021. 3
- [71] Bruno A Olshausen and David J Field. Emergence of simple-cell receptive field properties by learning a sparse code for natural images. *Nature*, 381(6583):607–609, 1996. 3
- [72] Keunhong Park, Arsalan Mousavian, Yu Xiang, and Dieter Fox. Latentfusion: End-to-end differentiable reconstruction and rendering for unseen object pose estimation. In *Proceedings of the IEEE/CVF conference on computer vision and pattern recognition*, pages 10710–10719, 2020. 3
- [73] Deepak Pathak, Philipp Krahenbuhl, Jeff Donahue, Trevor Darrell, and Alexei A Efros. Context encoders: Feature learning by inpainting. In *Proceedings of the IEEE conference on computer vision and pattern recognition*, pages 2536–2544, 2016. 3
- [74] Sida Peng, Yuan Liu, Qixing Huang, Xiaowei Zhou, and Hujun Bao. Pvnet: Pixel-wise voting network for 6dof pose estimation. In *Proceedings of the IEEE/CVF Conference on Computer Vision and Pattern Recognition*, pages 4561–4570, 2019. 1, 2
- [75] Giorgia Pitteri, Aurélie Bugeau, Slobodan Ilic, and Vincent Lepetit. 3d object detection and pose estimation of unseen objects in color images with local surface embeddings. In *Proceedings of the Asian Conference on Computer Vision*, 2020. 3
- [76] Fabio Poiesi and Davide Boscaini. Distinctive 3d local deep descriptors. In *2020 25th International conference on pattern recognition (ICPR)*, pages 5720–5727. IEEE, 2021. 3
- [77] François Pomerleau, Francis Colas, Roland Siegwart, et al. A review of point cloud registration algorithms for mobile robotics. *Foundations and Trends® in Robotics*, 4(1):1–104, 2015. 3
- [78] Georgy Ponimatkin, Yann Labbé, Bryan Russell, Mathieu Aubry, and Josef Sivic. Focal length and object pose estimation via render and compare. In *Proceedings of the IEEE/CVF Conference on Computer Vision and Pattern Recognition*, pages 3825–3834, 2022. 2
- [79] Marc’Aurelio Ranzato, Fu Jie Huang, Y-Lan Boureau, and Yann LeCun. Unsupervised learning of invariant feature hierarchies with applications to object recognition. In *2007 IEEE conference on computer vision and pattern recognition*, pages 1–8. IEEE, 2007. 3
- [80] Sachin Ravi and Hugo Larochelle. Optimization as a model for few-shot learning. In *International conference on learning representations*, 2017. 3
- [81] Ignacio Rocco, Mircea Cimpoi, Relja Arandjelović, Akihiko Torii, Tomas Pajdla, and Josef Sivic. Neighbourhood consensus networks. *Advances in neural information processing systems*, 31, 2018. 3
- [82] Ethan Rublee, Vincent Rabaud, Kurt Konolige, and Gary Bradski. Orb: An efficient alternative to sift or surf. In *2011 International conference on computer vision*, pages 2564–2571. Ieee, 2011. 3
- [83] Paul-Edouard Sarlin, Daniel DeTone, Tomasz Malisiewicz, and Andrew Rabinovich. Superglue: Learning feature matching with graph neural networks. In *Proceedings of the IEEE/CVF conference on computer vision and pattern recognition*, pages 4938–4947, 2020. 3
- [84] Jonathan Sauder and Bjarne Sievers. Self-supervised deep learning on point clouds by reconstructing space. *Advances in Neural Information Processing Systems*, 32, 2019. 3
- [85] Jianbo Shi et al. Good features to track. In *1994 Proceedings of IEEE conference on computer vision and pattern recognition*, pages 593–600. IEEE, 1994. 4
- [86] Karen Simonyan and Andrew Zisserman. Very deep convolutional networks for large-scale image recognition. *arXiv preprint arXiv:1409.1556*, 2014. 3
- [87] James Christopher Sims. *An implementation of Deep Belief Networks using restricted Boltzmann machines in Clojure*. University of Rhode Island, 2016. 3
- [88] Jake Snell, Kevin Swersky, and Richard Zemel. Prototypical networks for few-shot learning. *Advances in neural information processing systems*, 30, 2017. 3
- [89] Chen Song, Jiaru Song, and Qixing Huang. Hybridpose: 6d object pose estimation under hybrid representations. In *Proceedings of the IEEE/CVF conference on computer vision and pattern recognition*, pages 431–440, 2020. 2
- [90] Yongzhi Su, Mahdi Saleh, Torben Fetzter, Jason Rambach, Nassir Navab, Benjamin Busam, Didier Stricker, and Federico Tombari. Zebrapose: Coarse to fine surface encoding for 6dof object pose estimation. In *Proceedings of the IEEE/CVF Conference on Computer Vision and Pattern Recognition*, pages 6738–6748, 2022. 2, 3
- [91] Jiaming Sun, Zehong Shen, Yuang Wang, Hujun Bao, and Xiaowei Zhou. Loftr: Detector-free local feature matching with transformers. In *Proceedings of the IEEE/CVF conference on computer vision and pattern recognition*, pages 8922–8931, 2021. 3, 4
- [92] Jiaming Sun, Zihao Wang, Siyu Zhang, Xingyi He, Hongcheng Zhao, Guofeng Zhang, and Xiaowei Zhou. Onepose: One-shot object pose estimation without cad models. In *Proceedings of the IEEE/CVF Conference on Computer Vision and Pattern Recognition*, pages 6825–6834, 2022. 1, 3, 4

- [93] Martin Sundermeyer, Maximilian Durner, En Yen Puang, Zoltan-Csaba Marton, Narunas Vaskevicius, Kai O Arras, and Rudolph Triebel. Multi-path learning for object pose estimation across domains. In *Proceedings of the IEEE/CVF conference on computer vision and pattern recognition*, pages 13916–13925, 2020. [3](#)
- [94] Martin Sundermeyer, Zoltan-Csaba Marton, Maximilian Durner, Manuel Brucker, and Rudolph Triebel. Implicit 3d orientation learning for 6d object detection from rgb images. In *Proceedings of the european conference on computer vision (ECCV)*, pages 699–715, 2018. [2](#)
- [95] Bugra Tekin, Sudipta N Sinha, and Pascal Fua. Real-time seamless single shot 6d object pose prediction. In *Proceedings of the IEEE conference on computer vision and pattern recognition*, pages 292–301, 2018. [1](#)
- [96] Meng Tian, Marcelo H Ang, and Gim Hee Lee. Shape prior deformation for categorical 6d object pose and size estimation. In *Computer Vision—ECCV 2020: 16th European Conference, Glasgow, UK, August 23–28, 2020, Proceedings, Part XXI 16*, pages 530–546. Springer, 2020. [2](#)
- [97] Oriol Vinyals, Charles Blundell, Timothy Lillicrap, Daan Wierstra, et al. Matching networks for one shot learning. *Advances in neural information processing systems*, 29, 2016. [3](#)
- [98] He Wang, Srinath Sridhar, Jingwei Huang, Julien Valentin, Shuran Song, and Leonidas J Guibas. Normalized object coordinate space for category-level 6d object pose and size estimation. In *Proceedings of the IEEE/CVF Conference on Computer Vision and Pattern Recognition*, pages 2642–2651, 2019. [1](#), [2](#)
- [99] Qianqian Wang, Zhicheng Wang, Kyle Genova, Pratul P Srinivasan, Howard Zhou, Jonathan T Barron, Ricardo Martin-Brualla, Noah Snively, and Thomas Funkhouser. Ibrnet: Learning multi-view image-based rendering. In *IEEE Conference on Computer Vision and Pattern Recognition (CVPR)*, 2021. [6](#)
- [100] Xiaolong Wang and Abhinav Gupta. Unsupervised learning of visual representations using videos. In *Proceedings of the IEEE international conference on computer vision*, pages 2794–2802, 2015. [3](#)
- [101] Yilin Wen, Xiangyu Li, Hao Pan, Lei Yang, Zheng Wang, Taku Komura, and Wenping Wang. Disentangled implicit shape and pose learning for scalable 6d pose estimation. *arXiv preprint arXiv:2107.12549*, 2021. [2](#)
- [102] Yilin Wen, Hao Pan, Lei Yang, and Wenping Wang. Edge enhanced implicit orientation learning with geometric prior for 6d pose estimation. *IEEE Robotics and Automation Letters*, 5(3):4931–4938, 2020. [2](#)
- [103] Paul Wohlhart and Vincent Lepetit. Learning descriptors for object recognition and 3d pose estimation. In *Proceedings of the IEEE conference on computer vision and pattern recognition*, pages 3109–3118, 2015. [3](#)
- [104] Yu Xiang, Tanner Schmidt, Venkatraman Narayanan, and Dieter Fox. Posecnn: A convolutional neural network for 6d object pose estimation in cluttered scenes. *arXiv preprint arXiv:1711.00199*, 2017. [1](#), [2](#)
- [105] Yang Xiao, Xuchong Qiu, Pierre-Alain Langlois, Mathieu Aubry, and Renaud Marlet. Pose from shape: Deep pose estimation for arbitrary 3d objects. *arXiv preprint arXiv:1906.05105*, 2019. [3](#)
- [106] Jiayu Yang, Wei Mao, Jose M Alvarez, and Miaomiao Liu. Cost volume pyramid based depth inference for multi-view stereo. In *Proceedings of the IEEE/CVF Conference on Computer Vision and Pattern Recognition*, pages 4877–4886, 2020. [3](#)
- [107] Lin Yen-Chen, Pete Florence, Jonathan T Barron, Alberto Rodriguez, Phillip Isola, and Tsung-Yi Lin. inerf: Inverting neural radiance fields for pose estimation. In *IEEE International Conference on Intelligent Robots and Systems (IROS)*, 2020. [3](#)
- [108] Lin Yen-Chen, Pete Florence, Jonathan T Barron, Alberto Rodriguez, Phillip Isola, and Tsung-Yi Lin. inerf: Inverting neural radiance fields for pose estimation. In *2021 IEEE/RSJ International Conference on Intelligent Robots and Systems (IROS)*, pages 1323–1330. IEEE, 2021. [2](#)
- [109] Sergey Zakharov, Ivan Shugurov, and Slobodan Ilic. Dpod: 6d pose object detector and refiner. In *Proceedings of the IEEE/CVF international conference on computer vision*, pages 1941–1950, 2019. [1](#), [3](#)